Priority Report

Cancer Research

Synthetic DNA-Encoded Monoclonal Antibody Delivery of Anti–CTLA-4 Antibodies Induces Tumor Shrinkage *In Vivo*

Elizabeth K. Duperret[1], Aspen Trautz[1], Regina Stoltz[1], Ami Patel[1], Megan C. Wise[2], Alfredo Perales-Puchalt[1], Trevor Smith[2], Kate E. Broderick[2], Emma Masteller[2], J. Joseph Kim[2], Laurent Humeau[2], Kar Muthumani[1], and David B. Weiner[1]

Abstract

Antibody-based immune therapies targeting the T-cell checkpoint molecules CTLA-4 and PD-1 have affected cancer therapy. However, this immune therapy requires complex manufacturing and frequent dosing, limiting the global use of this treatment. Here, we focused on the development of a DNA-encoded monoclonal antibody (DMAb) approach for delivery of anti–CTLA-4 monoclonal antibodies *in vivo*. With this technology, engineered and formulated DMAb plasmids encoding IgG inserts were directly injected into muscle and delivered intracellularly by electroporation, leading to *in vivo* expression and secretion of the encoded IgG. DMAb expression from a single dose can continue for several months without the need for repeated administration. Delivery of an optimized DMAb encoding anti-mouse CTLA-4 IgG resulted in high serum levels of the antibody as well as tumor regression in Sa1N and CT26 tumor models. DNA-delivery of the anti-human CTLA-4 antibodies ipilimumab and tremelimumab in mice achieved potent peak levels of approximately 85 and 58 μg/mL, respectively. These DMAb exhibited prolonged expression, with maintenance of serum levels at or above 15 μg/mL for over a year. Anti-human CTLA-4 DMAbs produced *in vivo* bound to human CTLA-4 protein expressed on stimulated human peripheral blood mononuclear cells and induced T-cell activation in a functional assay *ex vivo*. In summary, direct *in vivo* expression of DMAb encoding checkpoint inhibitors serves as a novel tool for immunotherapy that could significantly improve availability and provide broader access to such therapies.

Significance: DNA-encoded monoclonal antibodies represent a novel technology for delivery and expression of immune checkpoint blockade antibodies, thus expanding patient access to, and possible clinical applications of, these therapies.
Cancer Res; 78(22); 6363–70. ©2018 AACR.

Introduction

Immune modulatory monoclonal antibodies (mAb), in particular antibodies targeting the immune checkpoint molecules CTLA-4 and PD-1, have shown unprecedented impact in the clinic for patients with multiple types of solid tumors (1). Antibodies targeting CTLA-4, ipilimumab, and tremelimumab, were the first of this class to enter clinical studies in patients with solid tumors in 2000. Ipilimumab, was the first therapy to improve both progression-free survival and overall survival in patients with melanoma, and was FDA approved for treatment of unresectable or metastatic melanoma in 2011 (1). Additional clinical trials are ongoing for both ipilimumab and tremelimumab as well as next-generation CTLA-4–blocking antibodies alone or in combination therapies for a variety of different malignancies (1).

Despite the success of these therapies in the clinic, the price tag may limit the availability of these life-saving drugs for underserved populations (2). The high price is due in part to the complexity of manufacturing mAbs, and the high doses at which they are required in patients (3). Approaches that could allow for less frequent delivery and more simple formulations might be very valuable.

The use of gene delivery technologies has been proposed for delivery of prophylactic or therapeutic mAbs for infectious disease and cancer (4–7). The major delivery methods investigated have been viral vectors, DNA plasmids and *in vitro* transcribed RNA. Because of a host of likely limitations, to date none of these platforms have been used to encode antibodies targeting the immune checkpoint inhibitors PD-1 or CTLA-4.

Here, we report the design and development of DNA-encoded mAbs (DMAb) expressing antibodies targeting CTLA-4 directly *in vivo*. We show that synthetic sequence optimized DMAbs targeting mouse CTLA-4 protein can be robustly expressed *in vivo*, have a reasonable and unique half-life and can drive protective antitumor immune responses *in vivo*. We further show that optimized DMAbs encoding ipilimumab and tremelimumab are potently expressed *in vivo*, bind to human regulatory T cells and activate human effector T cells. This strategy potentially provides a novel approach to immune checkpoint therapy, allowing for more novel and widely useful options for this technology in the management and treatment of cancer.

[1]The Wistar Institute, Vaccine and Immunotherapy Center, Philadelphia, Pennsylvania. [2]Inovio Pharmaceuticals, Plymouth Meeting, Pennsylvania.

Note: Supplementary data for this article are available at Cancer Research Online (http://cancerres.aacrjournals.org/).

Corresponding Author: David B. Weiner, The Wistar Institute, 3601 Spruce Street, Room 630, Philadelphia, PA 19104. Phone: 215-898-0381; Fax: 215-573-9436; E-mail: dweiner@wistar.org

doi: 10.1158/0008-5472.CAN-18-1429

Materials and Methods

Cell culture and transfection

HEK293T cells, CT26, and Sa1N tumor cells were obtained from the ATCC, which performs thorough testing and authentication of their cell lines using morphology, karyotyping, and PCR based approaches. They were maintained in DMEM supplemented with 10% FBS. They were both routinely tested for *Mycoplasma* contamination, and maintained at low passage (<20 passages) in cell culture. Only Sa1N or CT26 cells at lower than passage 5 were implanted into mice. HEK293T cells were transfected with GeneJammer transfection reagent according to the manufacturer's recommendations (Agilent). Cells and conditioned media were harvested 48 hours after transfection using RIPA lysis buffer (Cell Signaling Technology) containing EDTA-free protease inhibitor (Roche) for analysis by Western blot.

DNA plasmid construction

The amino acid sequences for 9D9, ipilimumab, and tremelimumab were obtained from published patents or available DrugBank sequences (US9868961B2 for 9D9). The nucleotide sequence for the mouse IgG2b (9D9) was codon optimized for mouse to enhance mammalian expression, and the nucleotide sequences for the human IgG1 (ipilimumab) and IgG2 (tremelimumab) were optimized for both mouse and human codon biases. All sequences were also RNA optimized and included a Kozak sequence. Plasmids were cloned into the modified pVax1 plasmid with a human cytomegalovirus promoter and bovine growth hormone polyA sequence (GenScript). Both heavy and light chains were encoded in the same plasmid, separated by a furin cleavage site (RGRKRRS) and a P2A peptide to ensure cleavage. Additional sequence modifications for 9D9 were made based on sequence alignment to the mouse germline IGHV1-19*01 sequence, and are indicated in Supplementary Fig. S1.

DMAb injection and mouse tumor studies

C57Bl/6, Balb/c and A/J mice were purchased from The Jackson laboratory. DNA plasmids were formulated with 12 U of hyaluronidase enzyme (Sigma-Aldrich) in 30 μL total injection volume. Formulated DNA plasmid was injected at one site (100 μg) in the tibialis anterior (TA) muscle, or at 4 sites (100 μg per site) in both TA muscles and quadriceps muscles. Following plasmid injection, the muscles were pulsed with two 0.1 Amp electric constant current square-wave pulses using the CELLECTRA-3P device (Inovio Pharmaceuticals). For tumor challenge studies, A/J or Balb/c mice were implanted subcutaneously with 10 million Sa1N tumor cells or 500,000 CT26 tumor cells, respectively, in PBS on the right flank. As human antibodies are immunogenic in immune competent mice, we studied their expression in Balb/c mice that were depleted of $CD4^+$ and $CD8^+$ T cells transiently at the time of DMAb injection (using a 200 μg injection of clone GK1.5 and clone YTS 169.4, BioXCell). For tumor studies, mice were euthanized when tumors reached 1.5 cm in diameter. All mice still alive at the end of study cleared their tumors completely. All animal studies were performed in accordance with guidelines from the National Institute of Health, and were approved by the Wistar Institutional Animal Care and Use Committee.

Human patient samples

Human blood was obtained from consenting adult healthy volunteers through the Wistar Phlebotomy core under Institutional Review Board–approved protocol #21801304. Written informed consent was obtained from all patients, and studies were conducted in accordance with recognized ethical guidelines (Delaration of Helsinki). Whole blood was collected in heparinized tubes and subsequently layered on top of an equal volume of histopaque 1083 (Sigma-Aldrich).

CTLA-4 blockade luciferase assay

T-cell activation after CTLA-4 blockade was assessed using the CTLA-4 Blockade Bioassay (Promega), according to the manufacturer's instructions. Ipilimumab and tremelimumab DMAb was purified from individual mice for this assay ($n = 3$ mice for each DMAb), using the Nab Protein A/G Spin Kit (ThermoFisher), and was concentrated using Amicon Ultra Centrifugal Filters (Millipore Sigma). Luciferase activity was measured using the Synergy2 plate reader (Biotek).

Statistical analysis

Statistical analysis was performed using GraphPad Prism software. Error bars represent the mean ± SEM or the mean ± SD, as indicated in the figure legend. Statistical significance was determined by a Student *t* test for experiments containing two experimental groups and by a one-way ANOVA, followed by Tukey *post-hoc* HSD test for experiments with more than two groups. For tumor growth over time, multiple *t* tests were performed for each time point. For mouse survival analysis, significance was determined using a Gehan–Brelow–Wilcoxon test. IC_{50} values were calculated using a non-linear regression of serum concentration versus OD450 value; *, $P < 0.05$; **, $P < 0.01$; ***, $P < 0.001$; ****, $P < 0.0001$.

Detailed methods related to Western blot, ELISA, immunofluorescence staining, and human peripheral blood mononuclear cell (PBMC) stimulation and staining are included in the Supplementary Methods.

Results

Design, expression and binding of mouse anti-mouse CTLA-4 DMAbs

We used the mouse anti-mouse CTLA-4 9D9 clone to encode in our optimized DNA expression system, based on its previously described antitumor activity (8, 9). The design for this DMAb plasmid was built off prior DMAb work from our group in the infectious disease space, and is described in detail in the Materials and Methods (4, 5).

Transfected HEK293T cells were able to produce and secrete 9D9 DMAb antibody *in vitro*, detected by ELISA and Western blot (Fig. 1A and B). However, expression of this DMAb was low (~660 ng/mL) compared with other previously examined DMAbs (4, 5). We therefore engineered several modifications into the DMAb to improve expression, including modification of the beginning and end of the heavy-chain sequence (Supplementary Fig. S1A and S1B). Although modification of the end sequence alone (mod #2) only slightly improved antibody production *in vitro*, modification of the beginning sequence or both sequences significantly improved antibody production, with nearly a 10-fold improvement in antibody secretion to the media for mod #4 (Fig. 1B). These framework modifications did not alter the binding to mouse CTLA-4 protein by ELISA, with similar IC_{50} values compared with recombinant 9D9 (range, 36.105–44.25 ng/mL; Fig. 1C).

We next tested expression of these DMAbs in C57Bl/6 mice through delivery by IM-EP (100 μg; Fig. 1D). Similar to the *in vitro*

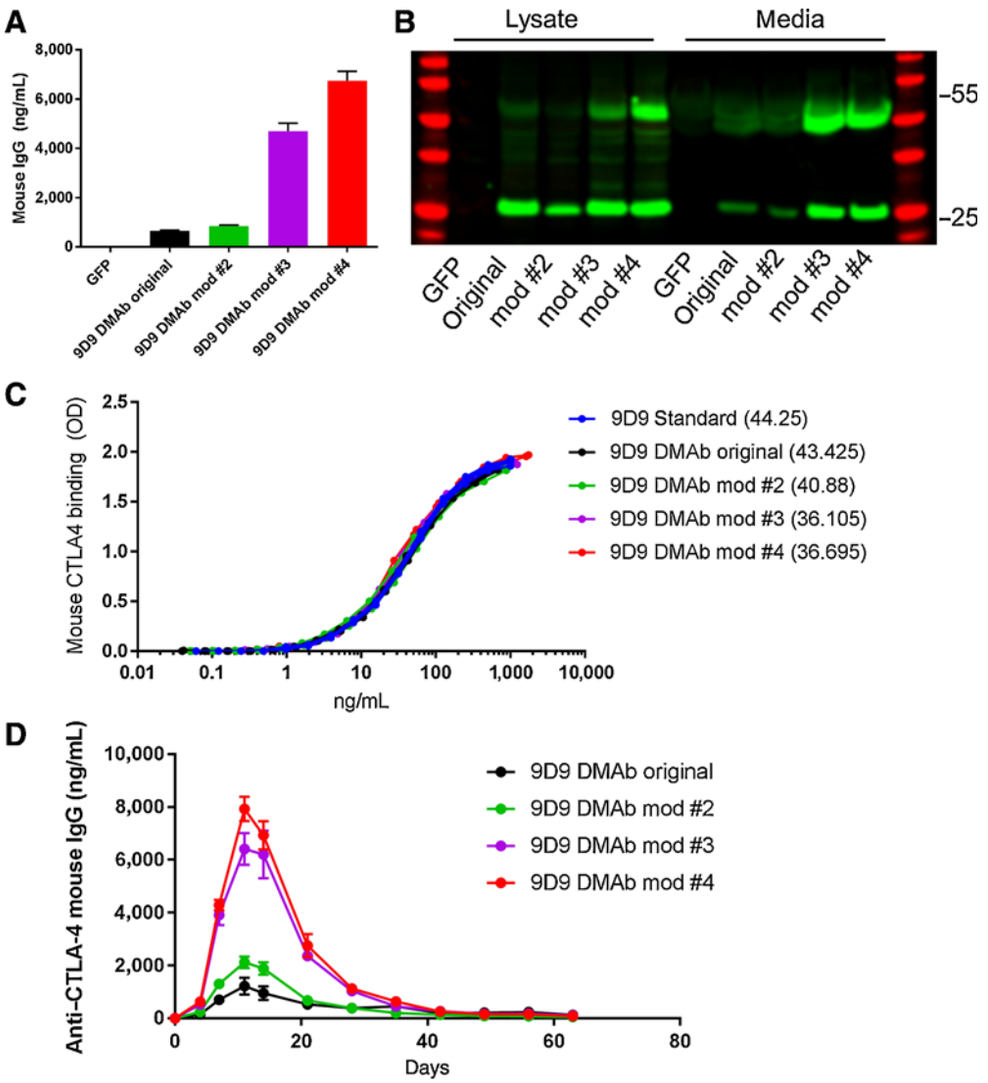

Figure 1.

Expression and binding of mouse anti-mouse CTLA-4 DMAbs. **A,** Secreted mouse IgG levels for the indicated DMAb from transfected HEK293T cells. **B,** Western blot of mouse IgG from lysates (left) and supernatants (right). Red bands, ladder; green bands, mouse IgG. **C,** Binding of purified 9D9 or supernatants from transfected cells to mouse CTLA-4 protein. IC_{50} is indicated in the legend. Individual curves from biological replicates are shown. **D,** Serum concentration of anti–CTLA-4 mouse IgG from C57Bl/6 mice injected with 100 μg of the indicated DMAb. Error bars indicate mean ±SD for *in vitro* studies and mean ± SEM for *in vivo* studies. **A** and **C,** n = at least two biological replicates. **D,** n = 5 mice per group.

results, the original 9D9 DMAb produced antibody in the serum at relatively low levels (~1.2 μg/mL of serum; Fig. 1D). All three modified DMAbs expressed at higher levels, with the mod #4 producing levels of approximately 7.9 μg/mL, over 6-fold higher than the original DMAb sequence (Fig. 1D). These important framework modifications, therefore, greatly improved both *in vitro* and *in vivo* expression of this DMAb without altering binding to mouse CTLA-4 protein.

Antitumor activity of anti-mouse CTLA-4 DMAb in multiple tumor models

We next studied the highest expressing 9D9 DMAb (9D9 DMAb mod #4) in mouse tumor challenge models. We first used the Sa1N fibrosarcoma model, which is one of the first models used to demonstrate antitumor immunity from CTLA-4 blockade (10). We compared antitumor activity of the 9D9 DMAb to that of the recombinant 9D9 antibody (Fig. 2A). Because DMAbs take a few days to be secreted from the muscle tissue, we started DMAb delivery 4 days earlier than recombinant 9D9. We compared one injection of DNA (400 μg) with three injections of recombinant 9D9 antibody, delivered 3 days apart (10 μg per injection), and observed similar kinetics of expression (Fig. 2A; Supplementary Fig. S2A and S2B), indicating prolonged duration of expression of the DMAb. Upon challenge with Sa1N tumor cells, both the 9D9 DMAb and the recombinant 9D9 were effective at inducing tumor clearance compared with control groups (Fig. 2B; Supplementary

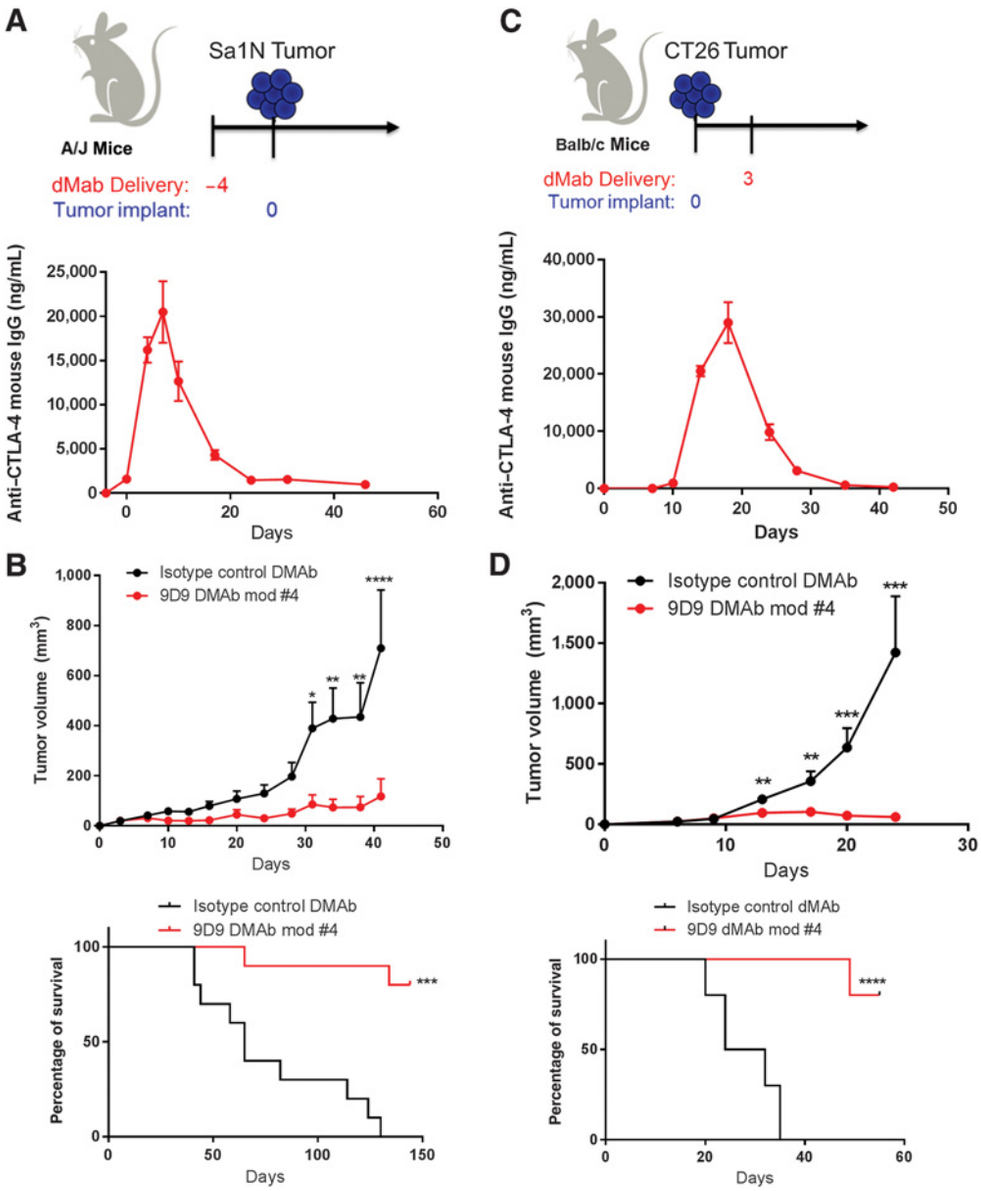

Figure 2.

Antitumor activity of anti–CTLA-4 DMAb in Sa1N and CT26 tumor models. **A,** Tumor study outline for DMAb delivery using prophylactic Sa1N tumor model in A/J mice (top), and serum levels of anti-CTLA-4 mouse IgG from these mice (bottom). Four hundred μg DMAb was delivered by IM-EP 4 days before implantation of tumor cells. **B,** Tumor volume measurements and survival analysis of the mice described in **A**. **C,** Tumor study outline for DMAb delivery using therapeutic CT26 tumor model in Balb/c mice (top), and serum levels of anti–CTLA-4 mouse IgG from these mice (bottom). Four hundred μg DMAb was delivered by IM-EP 3 days after implantation of CT26 tumor cells. **D,** Tumor volume measurements and survival analysis of the mice described in **C**. Error bars, mean ± SEM. $N = 10$ mice per group. Shown is a representative of two independent experiments.

Fig. S2C). Tumors grew in all mice initially upon implantation; however, upon DMAb delivery, 8/10 mice cleared their tumors (Fig. 2B). Upon recombinant 9D9 delivery, 9/10 mice completely cleared their tumors (Supplementary Fig. S2D). Because of the immunogenic nature of this tumor, 3/10 mice in the mouse IgG control group also cleared their tumors spontaneously (Supplementary Fig. S2D). To test for immunologic memory after DMAb exposure, we re-challenged the mice that cleared their tumors 6 months after the initial treatment (Supplementary Fig. S3). 100% of the mice that were previously treated with either recombinant 9D9 antibody or 9D9 DMAb cleared the re-implanted tumors (Supplementary Fig. S4). We also demonstrated that earlier DMAb administration (7 days before tumor implantation) was also effective at inducing tumor clearance in 6/10 mice (Supplementary Fig. S4A–S4C). In summary, anti-CTLA4 DMAbs exhibit prolonged serum antibody levels

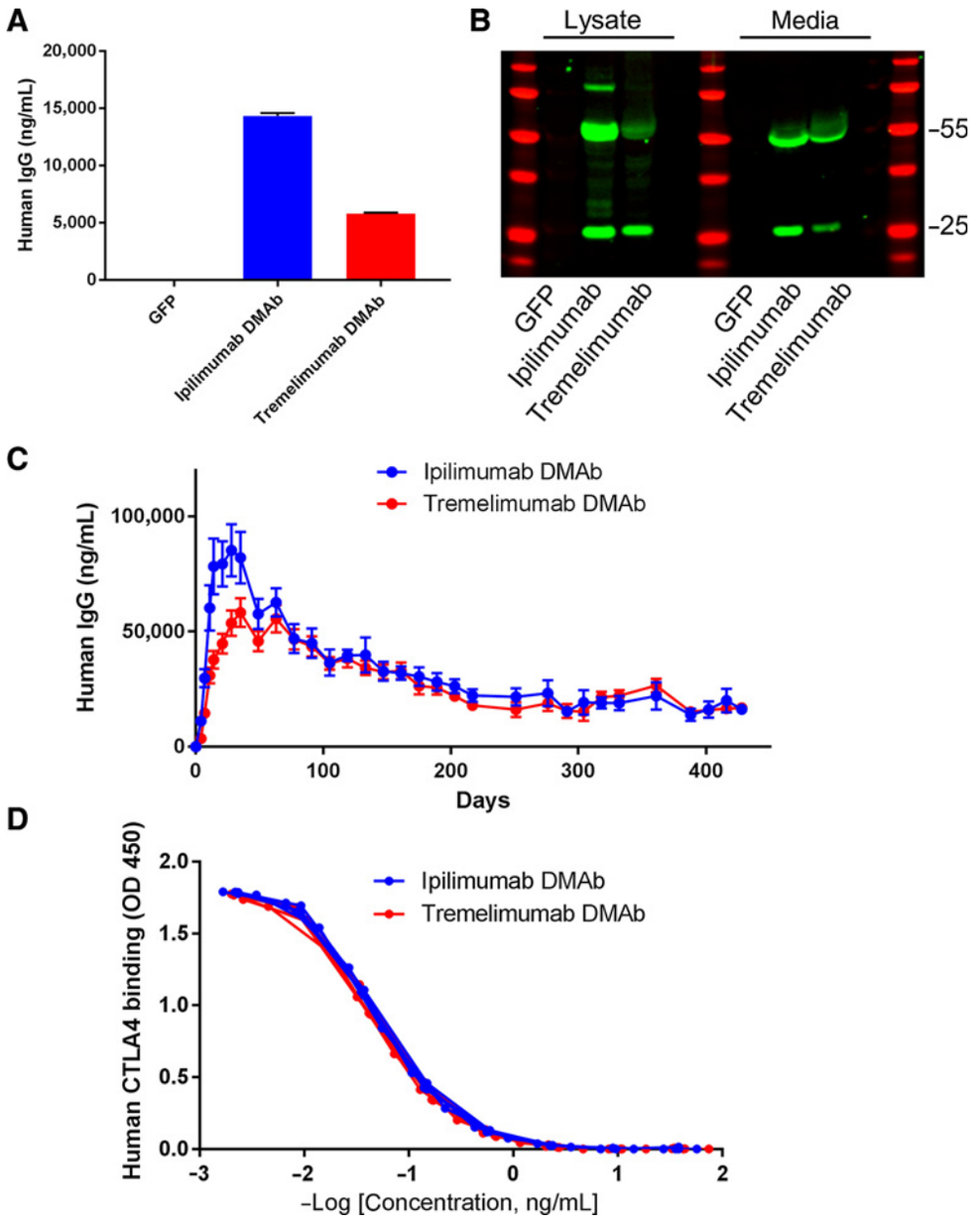

Figure 3.

Expression and binding of human anti-human CTLA-4 DMAbs. **A,** Secreted human IgG levels for the indicated DMAb from transfected HEK293T cells. **B,** Western blot of human IgG from lysates (left) and supernatants (right). Red bands, ladder; green bands, human IgG. **C,** Serum concentration of human IgG over time in Balb/c mice injected with 400 μg of the indicated DMAb by IM-EP. **D,** Binding of ipi-DMAb and treme-DMAb purified from mouse serum to human CTLA-4 protein by ELISA. Curves from individual mice are shown. For *in vitro* experiments, error bars indicate mean ±SD. For *in vivo* experiments, error bars indicate mean ± SEM. **A,** $n = 2$ biological replicates. **C,** $n = 5$ mice per group. **D,** $n = 3$ mice per group.

exhibiting an injection sparing effect with similar antitumor activity compared with recombinant mAb.

We next tested the impact of 9D9 DMAb on the tumor microenvironment before tumor clearance at day 10 (Supplementary Fig. S5A). At this early time point, tumors from both groups were similar sizes. The 9D9 DMAb induced higher levels of global lymphocyte infiltration ($CD3^+$ cells) as well as specifically $CD8^+$ T-cell infiltration, compared with isotype control mice, indicating potent immune stimulatory capacity driven by the DMAb (Supplementary Fig. S5B and S5C). In addition, the $CD8^+$ T cells infiltrating the 9D9 DMAb-treated tumors expressed higher levels of activation markers, including CD44, CD69, and PD1 (Supplementary Fig. S5D). Importantly, tumors treated with the 9D9 DMAb had a significantly lower proportion of regulatory T cells ($CD4^+/CD25^+/FoxP3^+$; Supplementary Fig. S5E).

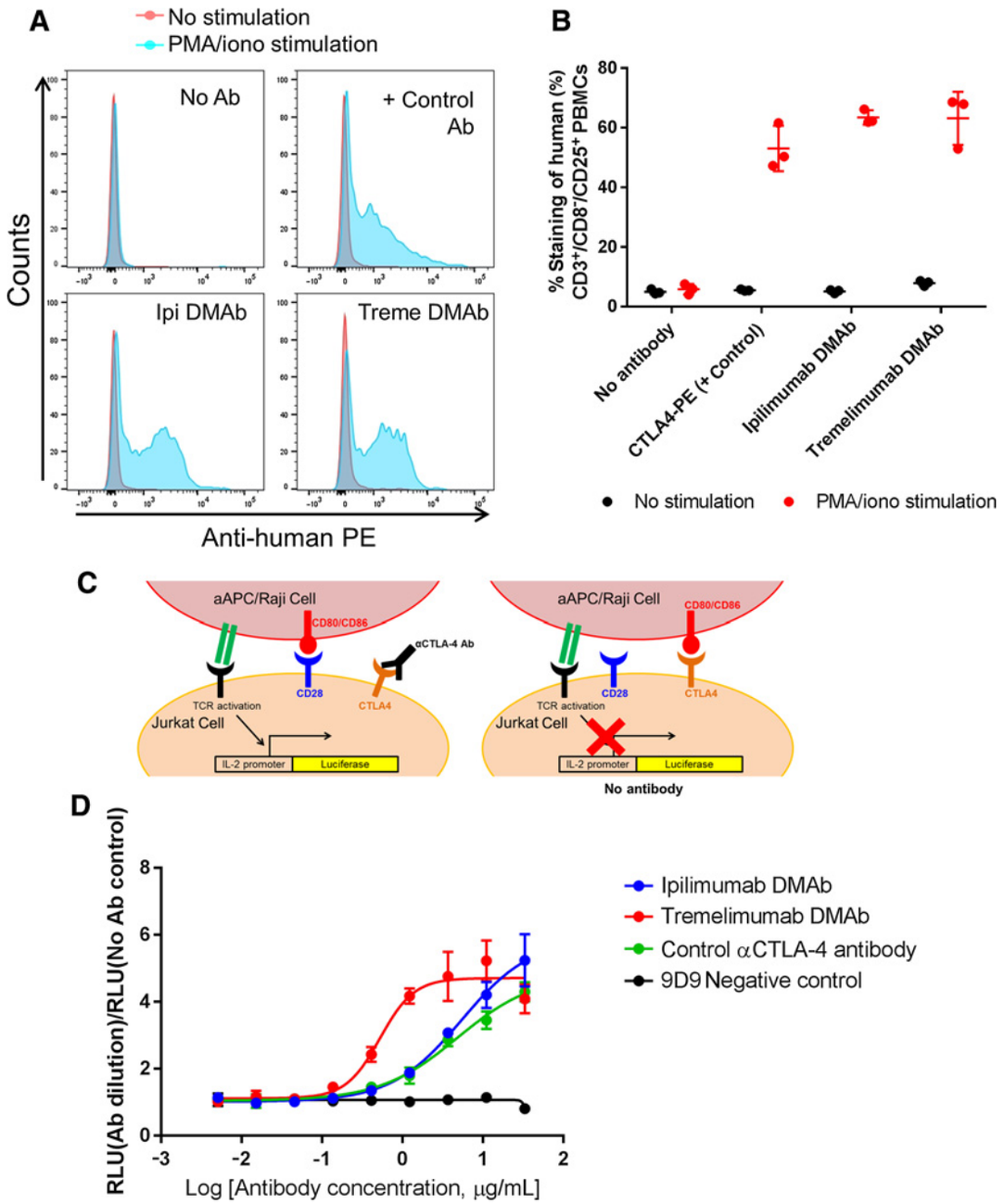

Figure 4.

Functionality of human anti-human CTLA-4 DMAbs. **A,** Flow cytometric staining of $CD3^+CD8^-CD25^+$ human PBMCs for CTLA-4 with the indicated antibodies, with or without PMA/ionomycin stimulation. **B,** Quantification of the staining depicted in **A** for three individual donors. **C,** Illustration of CTLA-4 blockade bioassay. **D,** Results from bioassay described in **C**. The relative luciferase units (RLU) are graphed relative to the RLU from no antibody control wells. Ipi-DMAb and treme-DMAb were purified from mouse serum. Error bars, ± SD. For **D**, curves indicate 4-parameter nonlinear fit.

We next tested the efficacy of this DMAb in a therapeutic setting in the CT26 tumor model. For this model, we began DMAb administration 3 days after tumor implantation (Fig. 2C). The 9D9 DMAb exhibited high expression in this mouse strain (Fig. 2C), and was effective at controlling tumor growth in this therapeutic setting, inducing tumor clearance in 8/10 mice (Fig. 2D). These results support the versatility of this DMAb platform across multiple mouse strains and tumor models.

Expression and binding of human anti-human CTLA-4 DMAbs

We next studied both *in vitro* and *in vivo* production of clinically relevant ipilimumab and tremelimumab DMAbs (ipi-DMAb and

treme-DMAb; Fig. 3). Both of these DMAbs were expressed and secreted at very high levels into the media of transfected cells *in vitro* (~14.3 μg/mL for ipi-DMAb and ~5.8 μg/mL for treme-DMAb, Fig. 3A). In addition, both heavy and light chains were clearly visible in both lysate and media by Western blot (Fig. 3B).

Dosing of 400 μg of formulated DNA in the tibialis anterior and quadriceps muscles of Balb/c mice demonstrated robust expression of both DMAbs, with potent peak expression levels of approximately 85 μg/mL for ipi-DMAb and approximately 58 μg/mL for treme-DMAb (Fig. 3C). These studies were done in mice depleted of CD4 and CD8 T cells to eliminate the anti-human immune response (Supplementary Fig. S6). Both DMAbs produced mAb for prolonged periods of over one year (Fig. 3C). Importantly, the DMAb harbored in the serum of the treated animals bound robustly to human CTLA-4 by ELISA (Fig. 3D).

Functionality of human anti-human CTLA-4 DMAbs

Functionality of the ipi-DMAb and treme-DMAbs was assessed using *in vitro* human T-cell assays (Fig. 4). PBMCs were isolated from three healthy donors, and stimulated with PMA/ionomycin to induce CTLA-4 surface expression on regulatory T cells (Fig. 4A; ref. 11). Because CD4 surface expression is downregulated upon stimulation with PMA/ionomycin, regulatory T cells (Treg) were classified as $CD3^+$, $CD8^-$, and $CD25^+$ PBMCs. Similar to the positive control anti-human CTLA-4 antibody, *in vivo* produced ipi-DMAb and treme-DMAb efficiently stained stimulated Tregs, but not unstimulated Tregs (Fig. 4A and B).

A functional T-cell activation assay was used to test the ability of the DMAbs to induce T-cell activation *in vitro*. For this assay, aAPC/Raji cells were coincubated with Jurkat cells that were transduced with a construct expressing luciferase off of the IL-2 promoter (Fig. 4C). Upon efficient blockade of the CTLA-4/CD80/CD86 interaction, these Jurkat cells can be efficiently activated and express luciferase (Fig. 4C). We found that ipi-DMAb, treme-DMAb and the positive control αCTLA-4 antibody induced luciferase expression in a dose-dependent manner (Fig. 4D). As expected, the negative control antibody (9D9) did not induce luciferase expression (Fig. 4D). Interestingly, the treme-DMAb induced luciferase expression at lower concentrations compared with the ipi-DMAb, potentially indicating more potent blocking function (Fig. 4D). Together, these results demonstrate that anti–CTLA-4 antibodies produced by DNA plasmids *in vivo* are functional.

Discussion

Here, we have described and validated a novel platform for the administration of immune checkpoint blockade antibodies through the use of DNA plasmids encoding IgG. The CELLECTRA electroporation approach described here has been widely used in clinical DNA vaccine trials, has a favorable safety and tolerability profile, and would be more rapid and cost efficient for mAb delivery compared with intravenous injection, which may broaden the applications that can be used for checkpoint antibodies (12, 13). In these pre-clinical studies, engineered DMAbs were efficient at driving *in vivo* expression of anti–CTLA-4 mAbs, and exhibited properties of IgG encoded CTLA-4 mAb. The DMAbs were capable of inducing potent antitumor immunity and CD8 T-cell infiltration while decreasing Treg infiltration. These results suggest that this technology could be used for novel therapeutic approaches that are currently limited for biologic mAbs, such as maintenance therapies.

Both DNA plasmid and viral delivery approaches have been used in pre-clinical models to deliver therapeutic mAbs for cancer therapy (14–16). However, these approaches thus far have focused on antibodies targeting cancer surface antigens or angiogenic factors. Although viral vectors can drive high expression, their use is limited to seronegative individuals, they can genetically mark patients, and they are difficult to re-administer due to seroconversion (7). Here, we report that the DMAb approach for immune checkpoint delivery can result in significant and prolonged *in vivo* expression from as little as a single dose.

Immune checkpoint blockade combination therapies are showing synergy in the clinic for certain indications (1). Although combination therapy between ipilimumab and nivolumab is highly effective in patients with melanoma, it also results in even more toxicity compared with monotherapy (17). Unfortunately, the full scope of this toxicity was difficult to predict using pre-clinical mouse or non-human primate models (18, 19). Because of this toxicity concern, next-generation versions of ipilimumab that can be selectively activated within tumors are currently being developed and tested in clinical trials (9, 20). Additional designs are being developed to enhance the effector function induced by these antibodies, including Fc mutations that enhance binding to the human FcγRIIIa as well as non-fucosylated versions with enhanced antibody-dependent cell-mediated cytotoxicity activity (9, 21). These important antibody improvements may provide expanded uses for CTLA-4–targeted antibodies in the future.

Additional areas for further development of this technology could include exploration of different isotypes to control function or expression *in vivo*, as well as new approaches for *in vivo* regulation of DMAb expression such as gene switch platforms that use small-molecule regulation as well as allosteric ribozymes (22–24). These interesting approaches could allow for self-regulation of therapy.

Using the DMAb platform, we have successfully delivered complex bi-specific antibodies, in addition to multiple different antibodies simultaneously within the same animal in the infectious disease arena (4, 5). This technology could therefore be adapted to include combination therapy with anti-PD1 DMAbs or with vaccines to open up additional therapeutic avenues. Further study of this novel approach is likely to provide valuable additions to the cancer therapy toolbox.

Disclosure of Potential Conflicts of Interest

M.C. Wise has ownership interest (including stock, patents, etc.) in Inovio Pharmaceuticals. T. Smith has ownership interest (including stock, patents, etc.) in and has provided expert testimony for Salary. K.E. Broderick has ownership interest (including stock, patents, etc.) in Inovio. E.L. Masteller is a senior director and has ownership interest (including stock, patents, etc.) in Inovio Pharmaceuticals. J.J. Kim is an employee and has ownership interest (including stock, patents, etc.) in Inovio. L. Humeau is SVP of R&D and has ownership interest (including stock, patents, etc.) in Inovio Pharmceuticals. K. Muthumani reports receiving a commercial research grant and is a consultant/advisory board member for Inovio Pharmaceutical. D.B. Weiner is in board service at Inovio and GeneOne, is a SAB, and reports receiving a commercial research grant from Inovio, GeneOne, Janssen, and Harbor, has ownership interest (including stock, patents, etc.) in Inovio, and is a consultant/advisory board member for Inovio, GeneOne, and Medimmune. No potential conflicts of interest were disclosed by the other authors.

Authors' Contributions

Conception and design: E.K. Duperret, A. Patel, J.J. Kim, K. Muthumani, D.B. Weiner

Development of methodology: E.K. Duperret, A. Trautz, A. Patel, M.C. Wise, A. Perales-Puchalt, T. Smith, K.E. Broderick, K. Muthumani

Acquisition of data (provided animals, acquired and managed patients, provided facilities, etc.): E.K. Duperret, A. Trautz, M.C. Wise, K.E. Broderick

Analysis and interpretation of data (e.g., statistical analysis, biostatistics, computational analysis): E.K. Duperret, A. Trautz, A. Perales-Puchalt, K.E. Broderick, E. Masteller, J.J. Kim

Writing, review, and/or revision of the manuscript: E.K. Duperret, M.C. Wise, A. Perales-Puchalt, K.E. Broderick, E. Masteller, L. Humeau, D.B. Weiner

Administrative, technical, or material support (i.e., reporting or organizing data, constructing databases): R. Stoltz, L. Humeau, K. Muthumani

Study supervision: L. Humeau, D.B. Weiner

Acknowledgments

This work was supported by an NIH/NCI NRSA Individual Fellowship (F32 CA213795 to E.K. Duperret), a Penn/Wistar Institute NIH SPORE (P50CA174523 to D.B. Weiner), the Wistar National Cancer Institute Cancer Center (P30 CA010815), the W.W. Smith Family Trust (to D.B. Weiner), funding from the Basser Foundation (to D.B. Weiner), and a grant from Inovio Pharmaceuticals (to D.B. Weiner).

Received May 11, 2018; revised August 16, 2018; accepted September 17, 2018; published first October 4, 2018.

References

1. Ribas A, Wolchok JD. Cancer immunotherapy using checkpoint blockade. Science 2018;359:1350–5.
2. Andrews A. Treating with checkpoint inhibitors-figure $1 million per patient. Am Heal drug benefits. Engage Healthcare Communications, LLC; 2015;8:9.
3. Ecker DM, Jones SD, Levine HL. The therapeutic monoclonal antibody market. MAbs 2015;7:9–14.
4. Elliott STC, Kallewaard NL, Benjamin E, Wachter-Rosati L, McAuliffe JM, Patel A, et al. DMAb inoculation of synthetic cross reactive antibodies protects against lethal influenza A and B infections. npj Vaccines 2017;2:18.
5. Patel A, DiGiandomenico A, Keller AE, Smith TRF, Park DH, Ramos S, et al. An engineered bispecific DNA-encoded IgG antibody protects against Pseudomonas aeruginosa in a pneumonia challenge model. Nat Commun 2017;8:637.
6. Muthumani K, Marnin L, Kudchodkar SB, Perales-Puchalt A, Choi H, Agarwal S, et al. Novel prostate cancer immunotherapy with a DNA-encoded anti-prostate-specific membrane antigen monoclonal antibody. Cancer Immunol Immunother 2017;66:1577–88.
7. Hollevoet K, Declerck PJ. State of play and clinical prospects of antibody gene transfer. J Transl Med 2017;15:131.
8. Selby MJ, Engelhardt JJ, Quigley M, Henning KA, Chen T, Srinivasan M, et al. Anti-CTLA-4 antibodies of IgG2a isotype enhance antitumor activity through reduction of intratumoral regulatory T cells. Cancer Immunol Res 2013;1:32–42.
9. Arce Vargas F, Furness AJS, Litchfield K, Joshi K, Rosenthal R, Ghorani E, et al. Fc effector function contributes to the activity of human anti-CTLA-4 antibodies. Cancer Cell 2018;33:649–663.
10. Leach DR, Krummel MF, Allison JP. Enhancement of antitumor immunity by CTLA-4 blockade. Science 1996;271:1734–6.
11. Jago CB, Yates J, Câmara NOS, Lechler RI, Lombardi G. Differential expression of CTLA-4 among T cell subsets. Clin Exp Immunol 2004;136: 463–71.
12. Trimble CL, Morrow MP, Kraynyak KA, Shen X, Dallas M, Yan J, et al. Safety, efficacy, and immunogenicity of VGX-3100, a therapeutic synthetic DNA vaccine targeting human papillomavirus 16 and 18 E6 and E7 proteins for cervical intraepithelial neoplasia 2/3: a randomised, double-blind, placebo-controlled phase 2b trial. Lancet 2015;386:2078–88.
13. Tebas P, Roberts CC, Muthumani K, Reuschel EL, Kudchodkar SB, Zaidi FI, et al. Safety and immunogenicity of an anti-Zika virus DNA vaccine—preliminary report. N Engl J Med. 2017 Oct 4. [Epub ahead of print]
14. Jiang M, Shi W, Zhang Q, Wang X, Guo M, Cui Z, et al. Gene therapy using adenovirus-mediated full-length anti-HER-2 antibody for HER-2 over-expression cancers. Clin Cancer Res 2006;12:6179–85.
15. Watanabe M, Boyer JL, Crystal RG. AAVrh.10-mediated genetic delivery of bevacizumab to the pleura to provide local anti-VEGF to suppress growth of metastatic lung tumors. Gene Ther 2010;17:1042–51.
16. Shi J, Liu Y, Zheng Y, Guo Y, Zhang J, Cheung P -t., et al. Therapeutic expression of an anti-death receptor 5 single-chain fixed-variable region prevents tumor growth in mice. Cancer Res 2006;66:11946–53.
17. Wolchok JD, Chiarion-Sileni V, Gonzalez R, Rutkowski P, Grob J-J, Cowey CL, et al. Overall survival with combined nivolumab and ipilimumab in advanced melanoma. N Engl J Med 2017;377:1345–56.
18. Keler T, Halk E, Vitale L, O'Neill T, Blanset D, Lee S, et al. Activity and safety of CTLA-4 blockade combined with vaccines in cynomolgus macaques. J Immunol 2003;171:6251–9.
19. Selby MJ, Engelhardt JJ, Johnston RJ, Lu L-S, Han M, Thudium K, et al. Preclinical development of ipilimumab and nivolumab combination immunotherapy: mouse tumor models, in vitro functional studies, and cynomolgus macaque toxicology. PLoS ONE 2016;11:e0161779.
20. Korman AJ, Engelhardt J, Loffredo J, Valle J, Akter R, Vuyyuru R, et al. Abstract SY09-01: next-generation anti-CTLA-4 antibodies. Cancer Res 2017;77:SY09-01-SY09-01.
21. Lazar GA, Dang W, Karki S, Vafa O, Peng JS, Hyun L, et al. Engineered antibody Fc variants with enhanced effector function. Proc Natl Acad Sci U S A 2006;103:4005–10.
22. Nomura Y, Zhou L, Miu A, Yokobayashi Y. Controlling mammalian gene expression by allosteric hepatitis delta virus ribozymes. ACS Synth Biol 2013;2:684–9.
23. Draghia-akli R, Malone PB, Hill LA, Ellis KM, Schwartz RJ, Nordstrom JL. Enhanced animal growth via ligand-regulated GHRH myogenic-injectable vectors. FASEB J 2002;16:426–8.
24. Burnside ER, De Winter F, Didangelos A, James ND, Andreica E-C, Layard-Horsfall H, et al. Immune-evasive gene switch enables regulated delivery of chondroitinase after spinal cord injury. Brain 2018;141:2362–81.